Acta Cryst. (1977). A33, 805–813

Multilayer Neutron Monochromators

BY A. M. SAXENA AND B. P. SCHOENBORN

Biology Department, Brookhaven National Laboratory, Upton, New York 11973, *USA*

(*Received* 14 *December* 1976; *accepted* 2 *April* 1977)

Thin-film multilayer monochromators have been fabricated and studied by neutron diffraction. Alternating thin films of two materials, such as Mn and Ge, constitute a one-dimensional crystal owing to the contrast in their scattering amplitude densities. The following are novel features of such a monochromator: (1) large and adjustable d spacing, (2) very high reflectivity, (3) adjustable bandwidth, $\Delta\lambda/\lambda$. Both kinematical and dynamical theories have been developed to give a proper understanding of the properties of a multilayer. Since a deviation from perfect periodicity can have a substantial effect on diffraction properties of a multilayer, a 'disorder factor' has been introduced in the dynamical theory. Finite resolution of the spectrometer has been taken into consideration when the experimental data are compared with the theoretical expressions. These multilayers can also be used as excellent polarizers and filters for neutrons.

With the development of the fission reactor in 1942, neutron beams of sufficient intensity could be produced to allow monochromatic diffraction studies. In these early experiments Zinn (1947) used a calcite crystal monochromator. Subsequently monochromators of lead, beryllium, copper, zinc and aluminum were used – unfortunately all of these exhibit low reflectivity. Only with the recent development of pyrolytic graphite by Riste & Otnes (1969) was an efficient low-energy neutron monochromator made available. These single-crystal monochromators can, however, only be used for wavelengths less than twice the unit-cell spacing, which is 6·7 Å for pyrolytic graphite. The use of these monochromators is also restricted by higher-order reflections ($\lambda/2$ *etc.*) which is particularly important at longer wavelengths.

In an earlier paper Schoenborn, Caspar & Kammerer (1974) reported the fabrication of a novel multilayer thin-film monochromator for neutrons. The 'multilayers' were made by alternately depositing thin films of two materials on a glass substrate. Such a system is periodic in the direction normal to the plane of the multilayer with a periodicity determined by the combined thickness of two films. If the materials chosen are such that their scattering parameters differ by a large amount, then a multilayer with a small number of bilayers can give rise to reflectivities comparable to pyrolytic graphite crystals. A detailed study of the multilayers has shown that they can be used as monochromators with unique properties. In addition to the high reflectivity, the diffracted beam has very low high-order contamination. Any multilayer of this kind will have a distribution of d spacings about a mean value which will roughly correspond to the mosaic distribution of a single crystal. The d spacing of such a monochromator can be anywhere between 40 and 250 Å with $\Delta\lambda/\lambda$ between 0·05 and 0·25. The width of the wavelength band reflected by the multilayer will be determined by the scattering angle, the thickness d and the distribution of d spacing, Δd. Since Δd can be easily increased while the multilayer is fabricated, it is possible to make a monochromator which gives rise to large bandwidth $\Delta\lambda/\lambda$ and increase the flux of incident neutrons if so desired.

The simplest approach for understanding the diffraction properties of the multilayers is to apply the kinematical theory. To allow comparison of these experiments with the observed properties, the effects of wavelength distribution and beam divergence for the spectrometer have to be taken into account. This will be described below, where a procedure similar to that of Cagliotti & Ricci (1962) will be followed. Since the multilayers have high reflectivities, dynamical effects will make a significant contribution. However, even a good multilayer is far from being a perfect crystal because of the disorder introduced during deposition, and the reflectivities are expected to be lower than those predicted by the dynamical theory for an ideal system. Therefore a 'disorder factor', similar to the Debye–Waller temperature factor, has been introduced. The value of the disorder factor has been calculated by comparing the theoretical reflectivity for a given sample with the experimentally observed reflectivity.

Multilayer preparation

The scattering parameter relevant to the choice of the materials for making a multilayer is the neutron scattering amplitude density, f, defined as $f=b\varrho$, where b is the scattering length per atom and ϱ is the number of nuclei per unit volume. Values of f for some materials are listed in Table 1. For a given number and thickness of bilayers, the scattered intensity will be greater for materials with a larger difference in their f values. The difference between the scattering densities can be increased by choosing one material with

Table 1. *Neutron scattering amplitude density for some elements*

Element	$b(10^{-12}$ cm)	$f(10^{11}$ cm$^{-2})$
Be	0·77	0·96
Al	0·35	0·21
Ti	−0·34	−0·19
Mn	−0·36	−0·29
Ni	1·03	0·94
Cu	0·79	0·67
Ge	0·84	0·37
Ag	0·61	0·36
Pb	0·96	0·32

a negative scattering length and the other with a positive scattering length. The materials selected should also form uniform thin films and should have small interdiffusion. On the basis of these considerations it was decided to make multilayers of manganese and germanium. Manganese is one of the few elements with a negative scattering length and the interdiffusion between Mn and Ge is fairly small.

The multilayers were made by depositing thin films of Mn and Ge on a flat glass substrate by the vacuum deposition technique (Chopra, 1969). In order to make large monochromators, sputtering techniques are now being used since a film of uniform thickness cannot be made over a large area with a point source employed in an evaporation system. Manganese and germanium were placed in boats of tantalum and graphite, respectively, and were evaporated in succession by resistive heating of the boats. Since manganese sublimes to the vapor phase, it was necessary to use a covered boat for it. The pressure during the evaporation process was about 1×10^{-6} torr. The thicknesses of the films were measured with a quartz crystal oscillator. The frequency of the crystal changed linearly with the mass deposited on the transducer. The oscillator actuated a shutter through an automatic control unit, thereby closing and opening it at preset values. While one material was being evaporated, the other was kept slightly below its melting point so that the time interval between depositing films was fairly small.

The properties of a multilayer are sensitive to the distribution of thicknesses of the bilayers; in a good multilayer these thicknesses should be identical within a few percent. This was achieved by keeping the evaporation rate fairly low, a typical value being 1 Å s^{-1}. At low evaporation rates the films are contaminated with some oxygen and carbon. The compositions of different sections of a multilayer were determined by Auger spectroscopy and the contamination was, in general, found to be less than 2%. These impurities change the average scattering density of a layer, leaving the diffraction properties of the multilayer unaltered. Most of the multilayers were made by evaporating on a substrate held at room temperature. The area of the substrates used was $2{\cdot}5\times15$ cm and they were kept about 70 cm from the boats to ensure uniformity in the thickness of each film. Multilayers were made with d spacings ranging from 120 to 240 Å and with up to 100 bilayers.

Kinematical theory

Let $\mathbf{K}$ be the incident wave vector and $\mathbf{K}'$ the scattered wave vector. For Bragg reflection from the multilayer, the scattering vector is

$$\mathbf{Q}=\mathbf{K}-\mathbf{K}'=\hat{\mathbf{z}}\,(4\pi\sin\theta/\lambda) \tag{1}$$

where θ is the angle of incidence of the neutron wave on the multilayer, $\hat{\mathbf{z}}$ is a unit vector perpendicular to the plane of the multilayer (as shown in Fig. 1), and λ is the wavelength of the neutron beam. Let q be the ratio of the reflected to the incident amplitude due to the entire multilayer and dq the contribution to the amplitude from a thin layer dz. Following the Fresnel zone construction of James (1962) we may write

$$\mathrm{d}q=\frac{\varrho b\lambda}{\sin\theta}e^{iQz}\mathrm{d}z\,,$$

where the exponential term appears as a result of the phase difference between the wave diffracted from the layer dz and the wave diffracted from the top of the multilayer. The amplitude due to the entire multilayer is

$$q=\frac{\lambda}{\sin\theta}\int f(z)e^{iQz}\mathrm{d}z \tag{2}$$

where the scattering amplitude density depends on z because of the alternating sequence of layers. If $d/2$ is the thickness of each layer then the periodicity of the structure is d. Since the lateral dimensions are unimportant, a unit cell of this structure may be assumed to be of unit area in the xy plane. The structure factor for the unit cell is

$$F=\int_{z=0}^{d}f(z)e^{iQz}\mathrm{d}z\,. \tag{3}$$

The diffracted amplitude may now be written in terms of the structure factor

$$q=\frac{\lambda F}{\sin\theta}\sum_{p=0}^{N-1}\exp\left(iQpd\right), \tag{4}$$

where N is the number of bilayers in the multilayer and p is the index of the bilayer. After performing the summation and then mutliplying q by its complex conjugate one obtains the following expression for the

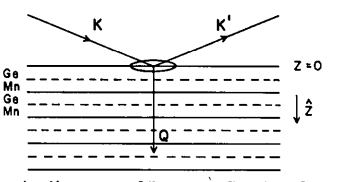

Fig. 1. Schematic diagram of Bragg reflection from a multilayer.

ratio of the diffracted intensity to the intensity incident on the multilayer:

$$|q|^2 = \frac{\lambda^2 |F|^2}{\sin^2\theta}\left[\frac{\sin(QNd/2)}{\sin(Qd/2)}\right]^2 . \quad (5)$$

This expression holds for a multilayer with a periodicity d, irrespective of the thicknesses of the films of the two materials. If these are identical and the boundary between the materials is sharp then the structure factor for this system may be obtained from equation (3):

$$|F|^2 = \left[\frac{\sin(Qd/4)}{Q}\right]^2 [f_1^2 + f_2^2 + 2f_1 f_2 \cos Qd/2] \quad (6)$$

for the nth order Bragg reflection $Q=(2\pi/d)n$ and equation (6) simplifies to

$$\begin{aligned} |F|_B^2 &= (d/n\pi)^2(f_1 - f_2)^2 \quad \text{for } n=1,3,5\ldots \\ &= 0 \qquad\qquad\qquad\quad \text{for } n=0,2,4\ldots . \end{aligned} \quad (7)$$

Therefore even-order reflections will be absent because the net diffracted intensity from each layer is zero. If $|F|^2$ is substituted in (5), the intensity of the nth-order Bragg reflection may be written as

$$|q|^2 = \left(\frac{4N^2d^4}{\pi^2 n^4}\right)(f_1 - f_2)^2 \quad n=1,3,5\ldots . \quad (8)$$

This shows that the reflectivity of a multilayer increases as the square of the number of bilayers and as the fourth power of its d spacing. This expression also shows that the reflectivity will decrease very rapidly with the order of reflection. It has been assumed in the above derivation that the films of the two materials are amorphous with a uniform distribution of nuclei. Since the multilayers are made in ordinary vacuum with very slow rates of deposition, it is highly unlikely that the films will have a definite crystalline order. This is supported by experimental observations. The multilayers do not show any high-angle reflection arising from the lattice spacings of Mn or Ge which shows that the films are either amorphous or polycrystalline with a very small grain size.

So far a sharp boundary between the materials has been assumed. For an actual multilayer, however, the boundary between the layers is not expected to be discrete because some diffusion takes place between the layers during evaporation. This has been confirmed by analyzing the composition of layers through Auger spectroscopy while the materials of the multilayer were removed by reverse sputtering. The high-order reflections are extremely weak for the multilayers; reflections of third and higher orders are almost nonexistent, which also suggests that some mixing of materials takes place.

For these reasons it is useful to calculate the reflected intensity for the case in which the scattering amplitude densities change continuously in a sinusoidal way. The partial scattering amplitude densities may then be written as

$$\begin{aligned} f'_1 &= \tfrac{1}{2}f_1(1+\sin gz) \\ f'_2 &= \tfrac{1}{2}f_2(1-\sin gz) , \end{aligned} \quad (9)$$

where $g=2\pi/d$. The structure factor of this bilayer is

$$\begin{aligned} F = \tfrac{1}{2}f_1 \int_0^d (1+\sin gz)\exp(iQz)\mathrm{d}z \\ + \tfrac{1}{2}f_2 \int_0^d (1-\sin gz)\exp(iQz)\mathrm{d}z \end{aligned} \quad (10)$$

which leads to

$$|F|^2 = \sin^2\frac{Qd}{2}\left[\frac{(f_1+f_2)^2}{Q^2} + \frac{g^2(f_1-f_2)^2}{(Q^2-g^2)^2}\right]. \quad (11)$$

For first-order Bragg reflection $Q=g=2\pi/d$. The first term of $|F|^2$ vanishes but the second term remains finite. By differentiation it can be shown that

$$\lim_{Q\to g}\left[\frac{\sin^2(Qd/2)}{(Q^2-g^2)^2}\right] = d^4/64\pi^2 .$$

Hence the structure factor for the first-order reflection is

$$|F|_B^2 = \tfrac{1}{16}d^2(f_1 - f_2)^2 \quad (12)$$

and $|F|^2$ is zero for all higher-order Bragg reflections. If equations (12) and (5) are combined, the reflectivity of the multilayer for the first-order reflection is

$$|q|^2 = \tfrac{1}{4}N^2d^4(f_1 - f_2)^2 . \quad (13)$$

Effect of finite resolution of the spectrometer

Characteristics of the multilayers were determined by taking θ–2θ plots and measuring their reflectivities. The observed angular variation of intensity will differ from $|q|^2$ because of the finite beam divergence and wavelength distribution of the spectrometer. General methods for introducing the effect of finite resolution of the spectrometer have been developed by Caglioti, Paoletti & Ricci (1960), Caglioti & Ricci (1962), Cooper & Nathans (1968) and other workers. However, a multilayer differs from a mosaic single crystal in some important aspects. In a single crystal each crystallite is assumed to be a perfect crystal with no definite phase relationship between waves diffracted from different crystallites. Since a multilayer with less than ten bilayers can give appreciable reflectivities, the intrinsic line widths become significant. In addition, the disorder in a multilayer is not equivalent to a mosaic distribution. Since the bilayers are stacked on each other, they are parallel and there is a definite phase relation in the waves diffracted by two bilayers. If a particular bilayer does not have the proper thickness, then it will affect the phase relation of the bilayers preceding and succeeding this bilayer.

An expression for a θ–2θ plot of a multilayer can be developed by following a procedure similar to that of Caglioti *et al.* (1960, 1962). The experimental setup is shown in Fig. 2. The incident neutron beam has

traversed a polycrystalline beryllium filter and therefore consists of a continuous distribution of wavelengths with a low-wavelength cutoff at 3·9 Å. The intensity of various wavelength components decreases uniformly from about 4 Å with negligible intensity for wavelengths greater than 7 Å. This distribution may be determined by taking a θ–2θ scan of the incident beam with a single crystal and applying suitable corrections for beam divergence. The wavelength composition of the primary beam is represented by $I_0(\lambda)$ and is assumed to be known.

The incident beam was collimated by allowing it to pass through two cadmium slits. For most of the experiments the beam width was 0·30 mm and the beam divergence was 1 m rad. The scattered beam from the sample was passed through Soller slits and was then reflected by a graphite analyzer into a ^{3}He detector. The appropriate wavelength was selected by adjusting the angular setting of the analyzer, and the wavelength distribution was determined by the mosaic spread of the analyzer.

The θ–2θ plot of a multilayer was obtained by aligning the multilayer and the Soller slits with the incident beam. The reflected intensity was measured for successive settings of the multilayer while the incremental angle for the detector arm was kept twice the angular displacement of the multilayer.

The intensity of the neutron beam reaching the detector for a given setting of the spectrometer and the multilayer is calculated by tracing the path of a general ray from the first collimating slit to the detector. To this general ray one assigns a probability for transmission or reflection through each element. The net probability of going through the spectrometer is the product of all these functions and the total intensity at the detector is obtained by integrating the probability function for all incident rays. The effect of vertical divergence will be neglected. It will also be assumed that the profile of the beam passing through the collimating slits is Gaussian, an assumption which is valid for the narrow slits used in these experiments. The distribution of mosaic blocks in the analyzer crystal is also represented by a Gaussian function.

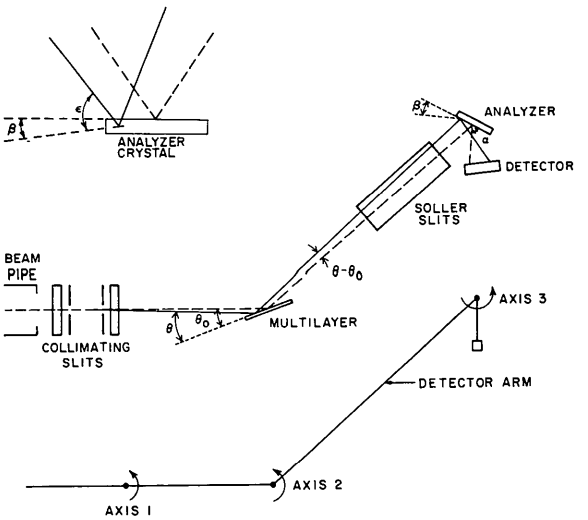

Fig. 2. Schematic diagram of the spectrometer. The upper inset shows a mosaic block of the analyzer which participates in reflection.

The constants K_1, K_2 and K_3 for the spectrometer, as defined in the list of symbols (Appendix), were experimentally determined by taking observations with a known configuration. The values ascribed to these constants were $K_1 = 2{\cdot}3678 \times 10^6$, $K_2 = 1{\cdot}6342 \times 10^5$ and $K_3 = 9{\cdot}4 \times 10^3$ rad^{-2}.

The probability function for a particular ray, as it passes through various reflectors and collimators, can be calculated in a straightforward way. The net intensity reaching the detector is then obtained by integrating the total probability so that it includes all possible rays. The integrated probability, $P(\theta_0)$, may be written as

$$P(\theta_0) = \int\int\int I_0(\lambda)\exp[-(K_1+K_2)(\theta-\theta_0)^2]|q(\theta)|^2 \times \exp(-K_3\beta^2)\delta(\lambda - 2d_G \sin\epsilon)\mathrm{d}\lambda\mathrm{d}\theta\mathrm{d}\beta\,. \quad (14)$$

The exponentials containing K_1, K_2, K_3 represent the attenuations introduced by the two collimators and the graphite analyzer respectively. $|q(\theta)|^2$ is the reflectivity of the multilayer for specular reflection at an angle θ, and is given by (5). $|F(\theta)|^2$ may be calculated from (6) or (11), depending on the assumptions made about the structure of a unit cell. It has been assumed that the particular ray is incident at an angle ϵ on the crystallite of the analyzer from which it is reflected. However, a crystallite of the analyzer reflects only that wavelength which satisfies the Bragg relation. This gives rise to the δ function in the integrand. It can be shown that $\epsilon = \alpha + \theta - \theta_0 + \beta$.

If a perfectly defined beam is incident on a multilayer with a finite number of bilayers, the diffracted beam will have some angular divergence. The effect of such non-specular reflections has been treated elsewhere (Saxena & Schoenborn, 1975). However, the effect of such reflections on the shape of the θ–2θ plots is not very significant and will not be considered here.

The integrations in (14) are performed over the following variables: (1) λ, to include the effect of wavelength distribution; (2) θ, to include the effect of beam divergence; (3) β, to include reflections from all orientations of the mosaic blocks in the analyzer. However, λ and β are related through the Bragg relation and only one of them is an independent variable. Therefore $P(\theta_0)$ may be written as

$$P(\theta_0) = \int\int I_0 \exp[-(K_1+K_2)(\theta-\theta_0)^2]|q(\theta)|^2 \times \exp[-K_3\beta^2]\mathrm{d}\lambda\mathrm{d}\theta \quad (15)$$

where

$$\beta=\sin^{-1}\left(\frac{\lambda}{2d_G}\right)+\theta_0-\alpha-\theta\,. \tag{16}$$

The observed angular variation of the intensity in a θ–2θ plot should be proportional to the angular variation of $P(\theta_0)$. The integrals of (15) were numerically evaluated using the Legendre–Gauss quadrature formula (see, for example, Hildebrand, 1956). A plot of $|q(\theta_0)|^2$ for $N=20$ and $d=160$ Å is shown as the thin line in Fig. 3 and the solid curve is $P(\theta_0)$ calculated from (15) with the constants of the spectrometer given earlier. $|q(\theta_0)|^2$ shows a number of oscillations between Bragg peaks, but these are smoothed out when the resolution of the spectrometer is taken into account.

Dynamical theory

According to the kinematical theory (equation 8) the reflectivity of a multilayer is proportional to the square of the number of bilayers in it. The straight line of Fig. 4 shows this dependence for a periodicity of 160 Å. The underlying assumption of the kinematical theory is that the intensity of the incident beam is uniform throughout the sample. Because of this assumption the reflectivity does not have an upper bound. Actually, however, the incident beam decreases in intensity as it goes deeper within the sample because part of it is reflected by the upper layers. In addition, a proper approach should consider multiple reflections inside the multilayer as well.

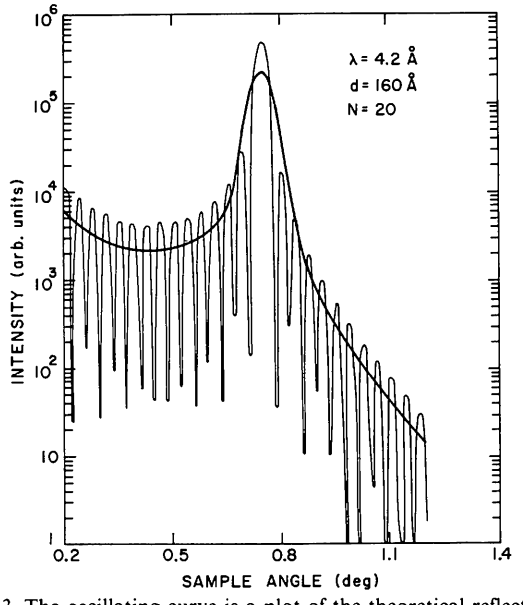

Fig. 3. The oscillating curve is a plot of the theoretical reflectivity, $|q(\theta)|^2$ *vs* half the scattering angle θ, for a sample with $N=20$ and $d=160$ Å. The heavy line is a plot of $P(\theta_0)$ as calculated from (15) for the same multilayer.

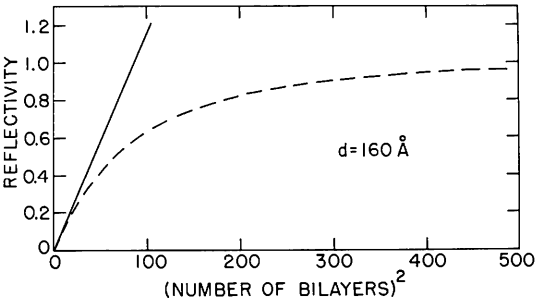

Fig. 4. Reflectivity for multilayers with $d=160$ Å according to dynamical theory (dashed curve) and also according to kinematical theory (solid line).

The reflectivity of a multilayer from the dynamical theory may be calculated by following a procedure similar to that of Zachariasen (1945) by replacing the X-ray constants with the appropriate constants for neutron diffraction. If I_0 is the intensity of the beam incident on the multilayer and I_B the intensity of the diffracted beam for a Bragg reflection, then

$$I_B/I_0=\tanh^2 A \tag{17}$$

where

$$A=2Nd^2(f_1-f_2)/n^2\pi\,. \tag{18}$$

The function I_B/I_0 is also plotted in Fig. 4 and it shows saturation as expected.

Disorder in multilayers

In the considerations so far it has been assumed that the multilayer is perfect in the sense that all the bilayers of a sample are of the same thickness. However, a single atomic layer of most materials is about 4 Å thick and all the samples will have some disorder built into them.

As mentioned earlier, if the thickness of a bilayer differs from d, then it makes a singular contribution to intensity and also alters the phase relation between waves diffracted from other bilayers. The diffraction properties of a multilayer will, therefore, depend on the thicknesses of all the bilayers and their stacking sequence. An exact approach will involve $2N$ unknown variables and will not be pursued here.

It will be assumed that the disorder is small and distributed over a large number of bilayers. A discrete disorder in one or two bilayers in the middle of the multilayer can give rise to very singular characteristics. For example, if the thickness of a bilayer in the middle of the multilayer is $d/2$, then one obtains a minimum of intensity at the Bragg angle. For a good multilayer the assumption that disorders are small and distributed seems to be appropriate. The effect of such disorders will be to reduce the reflectivity of the multilayer. The decrement in intensity may be incorporated in the dynamical theory by introducing a 'disorder factor' in analogy with the Debye–Waller temperature factor. One may then write

$$I_B/I_0=\exp(-\delta/N)\tanh^2 A \tag{19}$$

where δ is the disorder factor which measures the

average disorder in the bilayers. The effect of absorption in the bilayers has been neglected because the absorption cross section for Mn and Ge is fairly small. The reflectivities of the multilayers can approach 90%, which also suggests that absorption does not have an appreciable effect.

Experimental results

The beam divergence of the first collimator was kept at 1 mrad and that of the Soller collimator was 2·9 mrad. The analyzer was set to reflect neutrons of 4·2 Å into the detector. A typical θ–2θ plot for a sample with $N=25$ and $d=165$ Å is shown in Fig. 5. The first intensity maximum at 0·21° is due to critical-angle reflection from the glass substrate. A θ–2θ plot of the glass substrate alone will be identical with the multilayer plot from $\theta=0°$ to the intensity maximum at 0·21° but will show a sharp decrease of intensity above this angle. The multilayer does not intercept the entire beam for $\theta<0{\cdot}1°$ which accounts for the intensity minimum at $\theta\sim0{\cdot}1°$. The low-angle maximum can be eliminated by depositing the multilayer on a substrate made of a negative-scattering-length material such as titanium.

The first-order Bragg reflection for this sample occurs at 0·75°. The shape of this peak gives an indication of the quality of the sample. If the thicknesses of even a few bilayers are appreciably different from the d spacing of the lattice, then the Bragg peak will have prominent shoulders and may even be split into a number of maxima. The θ–2θ plot of such a sample with $N=37$ and $d=200$ Å is shown in Fig. 6.

The second-order reflection for this sample (Fig. 5) has an intensity about 1/200 of the intensity of the first-order reflection. Although this is a typical value for the ratio of first and second-order reflectivities, the actual ratio for a sample will depend on the amount of disorder and its distribution in the multilayer. Observed values of the relative reflectivity of the second order were found to span more than two orders of magnitude, from 1/10 to less than 1/1000. For most samples, third and higher orders were hardly distinguishable from the background.

Reflectivity of multilayers

The reflectivity of a multilayer was measured by mounting it on axis 1 (Fig. 2) such that the neutron beam was incident at the Bragg angle. A graphite crystal was mounted on axis 2 and the detector was set to receive neutrons directly after the Soller slits. A θ–2θ scan of the beam reflected by the multilayer was taken by stepping the graphite crystal and the detector in the ratio 1:2. This enabled a determination of the wavelength composition of the reflected beam. Next the multilayer was removed and the wavelength composition of the primary beam was determined by taking a θ–2θ scan again. The ratio of the intensities of the beam diffracted by the multilayer and the direct beam gave the reflectivity as a function of the wavelength of the neutron beam.

The reflectivities of various samples with $d=160$ Å and 220 Å and different number of bilayers are plotted in Fig. 7. These multilayers were made with almost identical evaporation rates and other parameters. The figure shows the results of dynamical theory with the disorder factor introduced earlier. The factor δ of (19) has been treated as a free parameter to get the best fit with the experimental data. The value assigned to the disorder factor for $d=160$ Å was 20·0, and for $d=220$ Å it was 8·0. The fact that a curve with one value of δ passes through the vicinity of a number of points shows that these multilayers have identical

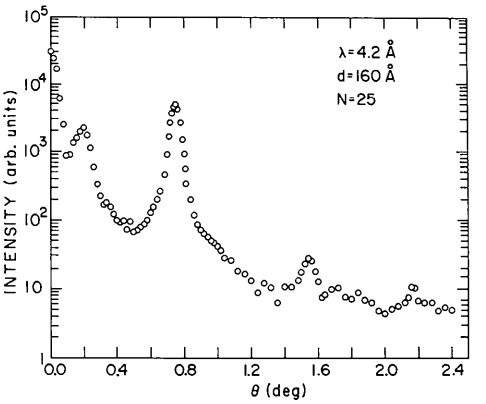

Fig. 5. Observed θ–2θ plot for a sample with $N=25$ and $d=160$ Å from an Mn–Ge multilayer. The analyzer was set for 4·2 Å wavelength.

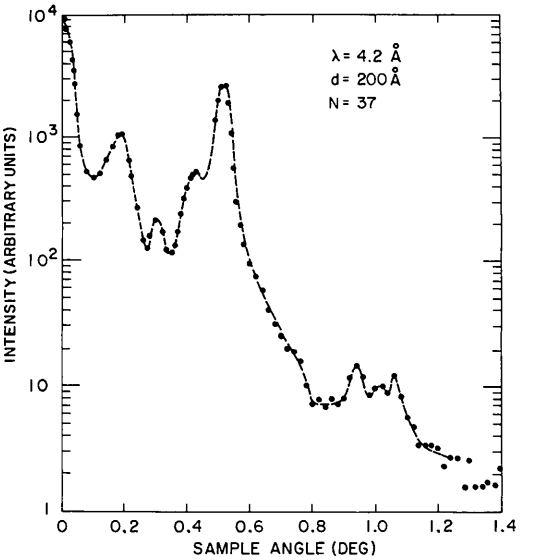

Fig. 6. Observed θ–2θ plot for a sample with large disorder, $N=37$ and $d=200$ Å. The dashed curve has been drawn through experimental data points and it shows a number of structures in the diffraction data.

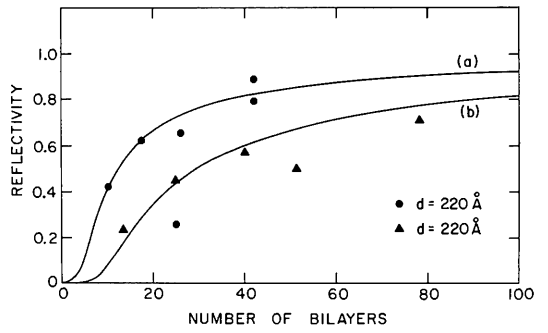

Fig. 7. Observed reflectivities of Mn–Ge multilayers compared with (19). Curve (*a*) is for $d=200$ Å and $\delta=8{\cdot}0$, and curve (*b*) is for $d=160$ Å and $\delta=20$. Solid circles represent reflectivities of samples with $d=220$ Å and triangles of those with $d=160$ Å. Points which deviate substantially from these curves represent multilayers with much greater disorder than the rest.

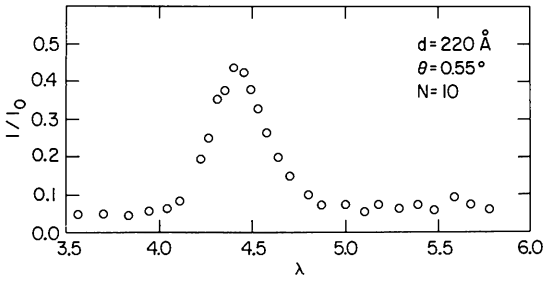

Fig. 8. Wavelength analysis of the beam reflected from a sample with $N=10$ and $d=220$ Å. It has been normalized with the wavelength distribution of the incident beam.

disorder. However a particular multilayer with any N and d may have substantially different disorder from the rest and will be far removed from the curve. It is also useful to remember that the effect of disorder has been introduced empirically in (19). A proper understanding of the properties of a multilayer will require a knowledge of the thicknesses of all the layers and their stacking sequence. Finally, surface irregularities of the substrate and nonuniformities in the surfaces of the films will also affect the reflectivity of a sample.

The observed values of bandwidths for the multilayer were between 0·08 and 0·20. If it is assumed that there is no disorder in the multilayer, it follows from Bragg relation that

$$\frac{\Delta\lambda}{\lambda}=(\cot\theta)\Delta\theta\,. \tag{20}$$

Substituting for $\Delta\theta$ the angular divergence of the beam, one finds the wavelength band, $\Delta\lambda$, reflected by a multilayer. For the experimental setup used in these experiments, $\Delta\lambda/\lambda=0{\cdot}76$ for $d=160$ Å. For a sample with disorder

$$\Delta\lambda/\lambda=(\cot\theta)\Delta\theta+\Delta d/d\,, \tag{21}$$

which shows that the wavelength band can always be made wider by introducing some aperiodicity in the multilayer during deposition. Fig. 8 shows a typical reflectivity plot for a sample with $\Delta\lambda/\lambda=0{\cdot}10$.

Interference of neutrons

This work on multilayers has also provided us with some unique data on the interference of neutrons. As shown in Fig. 3, the function $|q|^2$ oscillates between the Bragg peaks. These oscillations arise as a result of interference between waves diffracted from different bilayers of the samples. The minima of intensity occur when

$$QNd/2=r\pi\,, \tag{22}$$

where r is an integer not equal to 0, N, $2N$, *etc.* There will be $(N-1)$ minima between Bragg reflections of successive orders. The first of these minima ($r=1$) arises because the diffracted waves from the upper half of the multilayer destructively interfere with the diffracted waves from the lower half. A similar interpretation can be given to other minima of intensity.

If the period of oscillations is smaller than the beam divergence, the observed intensity does not show oscillations because it is integrated over more than a period. An attempt was made to observe these interference fringes by increasing the period of oscillation and decreasing the angular divergence of the incident beam. Since the period of oscillation for a sample is $\sim\lambda/2Nd$,

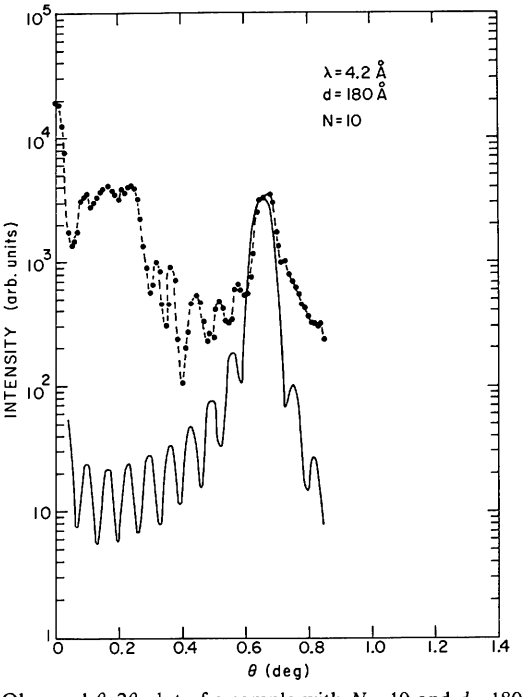

Fig. 9. Observed θ–2θ plot of a sample with $N=10$ and $d=180$ Å. The solid curve is the integral of $|q(\theta)|^2$ over beam divergence and wavelength distribution and represents the expected intensity variations in the θ–2θ plot of this multilayer. The dashed curve is obtained by joining the experimental data points and it clearly shows oscillations of the same frequency as the theoretical curve.

the total number of bilayers and the lattice spacing had to be decreased. However, decreasing Nd also decreases the intensity of reflections and a compromise had to be made to get observable intensities. The data shown in Fig. 9 were taken with a beam width of 0·06 mm and a beam divergence of 0·24 m rad. The sample had 10 bilayers with a d spacing of 180 Å. The θ–2θ plot clearly shows oscillations at the expected positions. Also shown is a plot of $P(\theta_0)$ of (15) which includes the effect of finite resolution. Recently interference of neutrons reflected from thin films has been observed by Hayter, Penfold & Williams (1976).

The observation of these interference fringes suggests that the coherence length of neutron wave packet is at least of the order of the total thickness of the multilayer. The conclusion from these observations is that the coherence length of a neutron wave packet is at least 0·2 μm. By observations of the diffraction pattern of a single slit, Shull (1969) has shown that the coherence length of the neutron wave packet was at least 0·3 μm.

Polarizing multilayers

Multilayers that polarize a beam of neutrons on reflection have also been made as reported by Lynn, Kjems, Passell, Saxena & Schoenborn (1976). For this purpose a multilayer with alternating layers of iron and germanium was constructed and placed in a magnetic field of about 300 Oe, which is enough to saturate the magnetization of iron. A multilayer with $N=32$ and $d=165$ Å was found to reflect 46% of the incident beam with 99% polarization. These figures suggest that efficient polarizers for neutrons can be made by using multilayers of this type. Recently Mezei (1976) has extended this idea for making 'supermirrors' which polarize and reflect neutrons of all wavelengths upto a certain critical value.

Multilayers as filters

In addition to being used as monochromators and analyzers, multilayers can also be used as filters for decreasing the intensity of the $\lambda/2$ component that gives rise to diffraction maxima at the same angle as the wavelength λ for which the spectrometer is set. Because the intensity of the second-order reflection is less than that of the first-order reflection by more than two orders of magnitude, a multilayer monochromator acts as a filter as well. Since the reflectivities of the multilayers can be up to 90%, it is possible to use them in series and get filtration of several orders of magnitude. Two such multilayers, with their reflecting sides facing each other, form a tunable filter where tuning to a particular wavelength is done by rotating the two with respect to the incident beam. It is also possible to deposit the multilayers on a material transparent to neutrons, such as quartz, and use them in tandem to remove any wavelength from the incident beam.

Discussion

Multilayers offer a number of advantages over conventional monochromators, particularly for experiments with long-wavelength neutrons. With the advent of cold moderators for neutrons, which give rise to low-energy neutrons, it is important to develop some monochromators which are effective at long wavelengths (6 to 20 Å). Multilayer monochromators have large and adjustable lattice spacings, high reflectivity and an adjustable band width. $\Delta\lambda/\lambda$ for the multilayers is large because of their smaller take-off angles and can be further increased by varying d during preparation. For applications in which a greater bandwidth is useful, such as low-angle scattering from biological samples, this leads to considerably greater intensities of the neutron beams.

One disadvantage of the multilayer is its size. Because of its greater d spacing, the neutron beam is incident at a smaller angle on a multilayer. In order to produce a reasonable beam size, the multilayer will have to be very long. For example, a multilayer with a d spacing of 80 Å will have to be 50 cm long in order to reflect a 12 mm wide beam of 4 Å wavelength neutrons. One solution of this problem is to make multilayers on a very thin substrate, such as mylar, and use them in parallel in 'Soller slit' geometry. However, with modern sputtering techniques it is possible to make multilayers with lattice spacing approaching 30 Å. There is a minimum thickness below which the films do not cover the substrate uniformly but form globules. This minimum thickness depends on the material chosen and the evaporation or sputtering conditions.

This research was carried out at Brookhaven National Laboratory, under the auspices of the United States Energy Research and Development Administration; with partial support of the NSF. The authors are indebted to Dr M. Strongin for his help in preparing the multilayers and to Drs L. Passell, F. Mezei and M. Blume for many useful discussions. The help given by Dr G. Zaccai at the early stages of this work is also gratefully acknowledged.

APPENDIX

List of symbols

K_1, K_2 Slit constants for the collimator defining the incident beam and the Soller slits before the detector, respectively. The probability of transmission of a ray making an angle θ with the axis of a slit is proportional to $\exp(-K_i\theta^2)$.

K_3 Constant determining the distribution of mosaic blocks in the analyzer such that the probability of finding a crystallite inclined at an angle β with the surface of the crystal is proportional to $\exp(-K_3\beta^2)$.

θ_0 Angle of incidence of the mean ray on the multilayer. The axis of the second collimator makes an angle $2\theta_0$ with the mean incident ray.

θ Angle of incidence of a particular ray on the multilayer.

α Angle of incidence of the mean ray on the analyzer.

β Angle subtended by the crystallite which reflects the particular ray with the surface of the analyzer.

ϵ Angle of incidence of the particular ray on the crystallite at an angle β with the surface of the analyzer.

d_G Lattice spacing of the analyzing crystal.

References

CAGLIOTI, C., PAOLETTI, A. & RICCI, F. P. (1960). *Nucl. Instrum. Meth.* **9**, 195–198.

CAGLIOTI, C. & RICCI, F. P. (1962). *Nucl. Instrum. Meth.* **15**, 155–163.

CHOPRA, K. L. (1969). *Thin Film Phenomena*, pp. 11–25. New York: MacMillan.

COOPER, M. J. & NATHANS, R. (1968). *Acta Cryst.* A**24**, 481–484.

HAYTER, J. B., PENFOLD, J. & WILLIAMS, G. (1976). *Nature, Lond.* **262**, 569–570.

HILDEBRAND, F. B. (1956). *Introduction to Numerical Analysis*, pp. 323–326. New York: McGraw Hill.

JAMES, R. W. (1962). *The Optical Principles of the Diffraction of X-rays*, pp. 34–41. London: Bell.

LYNN, J. W., KJEMS, J. K., PASSELL, L., SAXENA, A. M. & SCHOENBORN, B. P. (1976). *J. Appl. Cryst.* **9**, 454–459.

MEZEI, F. (1976). *Commun. Phys.* **1**, 81–85.

RISTE, T. & OTNES, K. (1969). *Nucl. Instrum. Meth.* **75**, 197–202.

SAXENA, A. M. & SCHOENBORN, B. P. (1975). *Brookhaven Symposia in Biology*, No. 27, VII-30–VII-48.

SCHOENBORN, B. P., CASPAR, D. L. D. & KAMMERER, O. F. (1974). *J. Appl. Cryst.* **7**, 508–510.

SHULL, C. G. (1969). *Phys. Rev.* **179**, 752–754.

ZACHARIASEN, W. H. (1945). *Theory of X-ray Diffraction in Crystals*, pp. 123–135. New York: John Wiley.

ZINN, W. H. (1947). *Phys. Rev.* **71**, 752–757.

Acta Cryst. (1977). A**33**, 813–818

Correction Factors for Neutron Diffraction from Lamellar Structures

BY A. M. SAXENA AND B. P. SCHOENBORN

Biology Department, Brookhaven National Laboratory, Upton, NY 11973, *USA*

(*Received* 28 *January* 1977; *accepted* 11 *April* 1977)

In a spectrometer with finite beam divergence the vertical size of the reflections will increase with the order of reflection. This effect will be more pronounced if the mosaic width of the sample is large, which is often the case with biological samples. When the size of the reflection is greater than the detector size, a correction factor has to be introduced to account for this loss of intensity. A method of calculating this correction factor for a given beam divergence and mosaic width has been developed.

In recent years a number of neutron diffraction studies on biological membranes have been reported. These membranes have a lamellar structure with d spacing ranging from 50 to 300 Å. Some of these systems show a high degree of crystalline order with mosaic spreads of less than 0·3° (FWHM) like that found in lecithin cholesterol (Blasie, Schoenborn & Zaccai, 1975; Schoenborn & Blasie, 1975; Worcester, 1976). Other membranes often do not have good orientation and mosaic spreads of up to 60° have been reported for retinal rods (Yeager, 1975; Chabre, Saibil & Worcester, 1975). In this paper we will study the effect of vertical divergence of the neutron beam on the intensities of Bragg reflections for a sample with large mosaic distribution.

The main spectrometer characteristics influencing the intensities of Bragg reflections are: the diffraction geometry (Lorentz factor), the wavelength bandwidth $\Delta\lambda$ and the beam divergence $\Delta\theta$. The Lorentz factor accounts for the fact that different sets of crystal planes do not have equal opportunity to diffract the incident beam. For single-crystal rotation techniques this factor is a measure of the relative amounts of time spent by the corresponding reciprocal-lattice point in passing through the Ewald sphere and is equal to $1/\sin 2\theta$ for lamellar samples when the rotation axis is normal to the plane containing the incident and scattered beam (Arndt & Willis, 1966) where θ is half the scattering angle. The effective wavelength bandwidth $\Delta\lambda$ is determined by the mosaic characteristic of the monochromator and the beam divergence $\Delta\theta$ depends on various collimating slits. The effect of these two will be to smear the Ewald sphere. A neutron spectrometer differs in two important aspects from an X-ray spectrometer. Since the neutron flux is much lower, one has to work with greater $\Delta\lambda$ and $\Delta\theta$ to get observable intensities for weak reflections. Second, the neutron beam is monochromatized by reflection from a single crystal which leads to a correlation between the wavelength and diffraction angle from the monochromator. The result of this is that the resolution will depend on the constants of the spectrometer, the scattering angle and also the characteristics of the sample.

In order to determine an unknown structure, one